Unraveling Hematopoietic Stem Cell Expansion: A Microfluidic 3D Co-culture Approach on Demineralized Bone Matrix

Amir Asri kojabad
Iran University of Medical Sciences
Maryam Atashbar
Bushehr University of Medical Sciences
Amir Atashi
Shahroud University of Medical Sciences
masoud soleimani
soleim_m@modares.ac.ir

Tarbiat Modares University

Research Article

Keywords: HSCs, MSCs Cord blood, microfluidic, 3D co-culture

Posted Date: April 9th, 2024

DOI: https://doi.org/10.21203/rs.3.rs-4107134/v1

Additional Declarations: No competing interests reported.

Abstract

Background

Hematopoietic stem cell transplantation (HSCT) is a well-established therapy for various hematological malignancies. Umbilical cord blood (UCB) HSCs offer an alternative source but are limited by a small number of CD34 + cells, delaying hematopoietic and immunologic recovery. Recent evidence underscores the importance of closely recapitulating the bone marrow niche for ex vivo stem cell expansion..

Methods

We describe a novel 3D microfluidic chip for dynamic co-culture of MSCs and HSCs within a demineralized bone matrix (DBM) scaffold. Co-culture was conducted in both dynamic and static 3D conditions without exogenous cytokines for seven days.

Results

Scanning electron microscopy images revealed that CD34 + CD38- cells primarily lodged beneath the MSCs layer rather than on its surface. MSCs repopulated the DBM scaffold and sustained HSC expansion for seven days. The proportion of CD34 + cells increased significantly (1.35-fold), with CD34 + CD38- cells nearly doubling in the microfluidic 3D co-culture compared to the control group. Microfluidic conditions promoted CXCR4 transcription (4.7-fold), colony-forming potency (3.6-fold), and osteogenic properties of DBM (9.4-fold) compared to the control group.

Conclusion

Indirect and direct crosstalk among HSCs, MSCs, and extracellular matrix (ECM) proteins can enhance UCB HSC expansion potency in an engineered bone marrow chip. Our microfluidic-based chip represents a significant step toward overcoming current limitations in UCB HSC numbers.

Background

Hematopoietic stem cells (HSCs) are pivotal for maintaining blood cell homeostasis and tissue regeneration throughout life(1–3). Hematopoietic stem cell transplantation (HSCT) stands as a cornerstone in cell-based therapies for various genetic, immunologic, or hematologic disorders(4). The success of HSCT is closely linked to the dose of CD34 + HSCs, which significantly impacts engraftment efficiency and reduces the risk of post-transplant infections(5)(6).

While peripheral blood, bone marrow, and cord blood serve as common sources of HSCs, umbilical cord blood (UCB) emerges as a promising alternative due to its ease of collection and immediate availability

of cryopreserved units(7)(8). Additionally, UCB exhibits a reduced risk of graft-versus-host disease (GVHD) owing to its naive immune system(9). However, the limited number of hematopoietic stem and progenitor cells (HSPCs) in a single unit of UCB presents a major obstacle, particularly for adult transplantation, leading to delayed engraftment and lower transplant success rates(10)(11).

Several strategies have been explored to address these limitations(12), including double-unit cord blood transplantation (DUCBT) (13) and optimization of conditioning regimens(14, 15). Despite these efforts, the expansion of cord blood HSCs ex vivo holds significant promise for enhancing transplant outcomes. However, conventional methods employing cytokine cocktails have proven inadequate due to their non-physiological concentrations and rapid differentiation of HSPCs(16).

The emergence of co-culture techniques and advancements in understanding HSC biology offer novel avenues to overcome these challenges. By replicating the hematopoietic microenvironment ex vivo, researchers aim to modulate the balance between HSC self-renewal and differentiation. Mesenchymal stem cells (MSCs) play a pivotal role in this niche, secreting factors that support HSC function and regulating their quiescence(17–19). Moreover, the extracellular matrix (ECM) produced by stromal cells provides structural support and signaling cues essential for HSC maintenance and expansion(20). Integrating microfluidic technology with 3D culture systems offers a promising approach to mimic the complex interplay between cells and their microenvironment. It was shown that MSCs-derived ECM enhances HSCs expansion capacity (21).

The interstitial flow in HSCs microenvironments delivers oxygen, nutrients, growth factors, and cells to niches of HSCs, as well as removing metabolic waste products(22). Traditional flask cell culture is not sufficient to mimic the complexity of interstitial flow in vitro due to its static nature. High-throughput microfluidic technology is a study of fluid flow through laminar flow micro-channels. Microfluidic based culture methods have been widely developed in the past few years. Continuous laminar flow perfusion has maintained controlled culture conditions that conventional static culture(23). Torisawa et al. established the first attempts to simulate a niche. Their results showed that microfluidic systems are capable of culturing HSCs in an engineered niche(24). Microfluidic culture systems can integrate with the 3D culture. Using scaffolds reduces the gap between engineering and in vivo niches. Although various scaffolds have been used for mimicking bone marrow to date, none have mimicked a niche three-dimensional microenvironment(8, 25, 26). Sieber and et al. describe a microfluidic-based 3D co-culture model based on a hydroxyapatite-coated zirconium oxide ceramic scaffold(27). We demonstrated that Microfluidic could be used to co-culture of HSCs with MSCs for seven days. It has been shown that MSCs can be promoted HSCs expansion by the secretion of soluble factors such as cytokines(28). In traditional expansion culture systems, cytokines were added to the culture medium. Co-culture of HSCs and MSCs in the absence of exogenous cytokines is one step closer to the bone marrow on-chip concept(29, 30). Numerous studies in both 3D and 2D cultures have confirmed that stromal cells in the co-culture model ensure cytokines' secretion (29).

In vitro niche architecture engineering is a challenging approach; the recent advanced shows that naturally occurred HSCs niches can be mimicked in vitro(27, 31, 32). Engineered niches allow for modifications of HSCs fate direction in a controlled manner. Dynamic co-culture of HSCs and MSCs on natural demineralized bone matrix (DBM) scaffold, enabling improving the number of $CD34^+$ $CD38^-$ HSCs in dynamic 3D culture. DBM is a natural-based allograft product produced by acid extraction of the bone allograft. DBM contains type I collagen (93%) and non-collagenous proteins, including osteogenic factors (such as bone morphogenetic proteins (BMPs), osteocalcin, Osteopontin, and growth and differentiation growth factors), as well as other naturally present molecules(33).

Here, we present a novel microfluidic-based 3D co-culture model utilizing DBM scaffolds in a cytokine-free microenvironment. By recapitulating the bone marrow niche ex vivo, this approach holds the potential to enhance the expansion of CD34 + CD38- HSCs, thus addressing the critical need for improved transplant outcomes in clinical settings.

METHODS

Microfluidic device fabrication

The microfluidic device fabrication process involves two main steps. Firstly, CAD design software (AutoCAD 2017) is utilized to draw the channel and main culture chamber. The molding is then created using computer numerical control (CNC) machining (ROTEC). In the subsequent step, the microfluidic device is fabricated through standard soft lithography. Polydimethylsiloxane (PDMS) (Sylgard 184 silicone elastomer) is mixed with a curing agent at a ratio of 10:1.05 w/w. This mixture is then poured onto the CNC-created mold (see Fig. 1a). The PDMS layer is assembled onto a glass slide using O2 plasma (ETP). After being exposed to a 70% ethanol solution for 30 minutes to clean the channels, the device is sterilized by UV light exposure for 20 minutes.

The culture chamber has a volume of 98 cubic centimeters, with inlet and outlet channels measuring 500 micrometers in dimension. The inlet and outlet are punched using a BPP-15F puncher from Kai Industries Co., Ltd., Seki, Japan. The inlet is connected to a syringe pump (JMS) via a tube. In the 3D dynamic group co-culture, the perfusion flow through the medium is precisely controlled at a rate of 1.6 µl min − 1. Specifically, a speed of 1.6 µl min − 1 per hour is set for the hematopoietic stem cells (HSCs), while a speed of five µl min − 1 per hour is set for mesenchymal stem cells (MSCs) (see Fig. 1b).

Stem cell isolation and cell culture

Mesenchymal stem cells (MSCs) were sourced from Bon-Yakhteh (Tehran, Iran). The expression of MSC surface markers was characterized using flow cytometry. MSCs were expanded for 3–5 passages in Dulbecco's Modified Eagle Medium (DMEM, Gibco), supplemented with 10% fetal bovine serum (FBS, Gibco), and 1% penicillin-streptomycin (Pen/strep, Sigma-Aldrich). Cultures were maintained at 37°C in a humidified atmosphere containing 5% CO2. MSCs used in culture experiments were between passages 3 to 5, and medium replacement was performed every three days. The osteogenic and adipogenic

differentiation potential of MSCs was assessed as previously described(34). After three weeks of culture in osteogenic medium, calcium deposition was determined by alizarin red staining, while differentiation into adipocytes was demonstrated by Oil red staining.

Fresh cord blood cells were obtained from the Iranian Blood Transfusion Organization (IBTO) with donors' consent. Umbilical cord blood (UCB) mononuclear cells were separated by a Ficoll density gradient (GE Healthcare) and centrifuged to deplete red blood cells, platelets, and plasma (400 g, 20 min). CD34 + cord blood hematopoietic stem and progenitor cells (HSPCs) were isolated using the CD34 MicroBead Kit, human (Miltenyi Biotec), according to the manufacturer's protocol. Harvested cell viability was analyzed using trypan blue (Bioidad) dye. Cells were stained for CD34 cell surface marker (eBioscience; FITC-conjugated CD34), and CD34 expression was analyzed by flow cytometry.

Co-culture experiment design

The co-culture of mesenchymal stem cells (MSCs) and hematopoietic stem cells (HSCs) was conducted in three groups: a 3D dynamic co-culture group performed on a microfluidic device (3D dynamic group), a 3D static co-culture group on 24-well plates (3D static group), and a conventional 2D co-culture group (2D static group) as the control (see Fig. 2E). The demineralized bone matrix (DBM) used in the study was purchased from Iranbaft (Iranian Tissue Bank) and was cylindrical in shape. In all 3D culture conditions, the DBM served as a 3D scaffold. The DBM was cut into cubes measuring 2×2×2 mm per well. Cells were seeded into the scaffolds using pipetting techniques. The scaffold was further divided into different pieces using a sterile Surgical Blade (Morris). One piece of DBM was utilized for each 3D dynamic and 3D static group. The DBM was embedded within the microfluidic device chamber before the plasma oxygen treatment of the device. Additionally, one piece of DBM was immersed in DMEM medium supplemented with 10% FBS, 100 U/ml penicillin, and 100 µg/ml streptomycin in a 24-well plate as a control.

Cell seeding

For the 3D dynamic group, cell seeding was conducted as follows: Initially, mesenchymal stem cells (MSCs) at a density of 100,000 cells were cultured for three days. Subsequently, 50,000 hematopoietic stem cells (HSCs) were injected into the microfluidic device. In the 24-well dynamic group, MSCs were seeded at a density of 20,000 cells per well onto the demineralized bone matrix (DBM) scaffold. On day 3, 10,000 CD34 + cells per well were added to the 3D static cell culture experiment, followed by a half medium exchange with serum-free Stemline II HSC media under cytokine-free conditions. HSCs and MSCs were co-cultured in a 5% CO2 atmosphere at 37°C for seven days.

In the 2D static control group, a co-culture experiment without the DBM scaffold was conducted in 24-well plates. The medium exchange was performed every three days. Before seeding HSCs, the culture medium was exchanged with the HSC expansion medium.

Harvesting cells

The cells from each demineralized bone matrix (DBM) scaffold were harvested by treating with Collagenase 0.01% (Biochrom) in phosphate-buffered saline (PBS) supplemented as described. After treatment, the harvested cells were centrifuged at 300g for 10 minutes. The viability of the cells was determined using trypan blue stain (0.4%) for 3 to 5 minutes.

RT-PCR

Gene expression analysis was conducted to quantify the mRNA expression of CXCR4 and RUNX2 genes on day seven of co-culture. Total RNA was isolated from the experimental groups using TRIzol Reagent (Invitrogen) following the manufacturer's instructions. The quality and quantity of total RNA were assessed using NanoDrop Spectrophotometers (Thermo Fisher Scientific). Subsequently, RNA was converted to cDNA using the Revert Aid first-strand cDNA synthesis kit (Fermentas) according to the manufacturer's protocol.

Real-time PCR was performed using SYBR Green Master Mix (Thermo Fisher) on the Step-One Plus real-time PCR system. Melting curve analysis was conducted to confirm the specificity of PCR amplification. The genes and their specific primers used in the analysis are detailed in Table 1. Each PCR reaction was repeated three times, and the average threshold cycle (Ct) value was used for data analysis. The fold change in gene expression was calculated using the $\Delta\Delta$Ct method.

Table 1
Primers sequences of CXCR4 and RUNX2 genes.

Sequence	Gene
CGC CACCAACAGTCAGAG	H CXCR4(F) Both variants
AAACAACCACCCACAAGTC	H CXCR4(R) Both variant
GCCTTCAAGGTGGTAGCCC	H RUNX2(F)
CGTTACCCGCCATGACAGTA	H RUNX2(R)
ATGGGGAAGGTGAAGGTCG	H-GAPDH-F
TAAAAGCAGCCCTGGTGACC	H-GAPDH-R

Scanning electron microscopy (SEM)

The morphology and physical interaction of hematopoietic stem cells (HSCs) and mesenchymal stem cells (MSCs) were visualized using scanning electron microscopy (SEM). The demineralized bone matrix (DBM) scaffold was initially fixed in 4% glutaraldehyde (Sigma) for 1 hour at 22°C, followed by overnight fixation at 4°C. Subsequently, the fixed specimens were dehydrated using a series of ethanol solutions, as described previously(35).

After dehydration, the samples were coated with gold and visualized using a Hitachi S-520 SEM. This technique allowed for high-resolution imaging of the surface morphology and physical interactions

between HSCs and MSCs within the DBM scaffold.

Colony-forming unit (CFU) assays

The colony-forming ability of the harvested cells, following the 7-day co-culture, was assessed using the MethoCul H4434 kit (STEMCELL Technologies). In brief, 1,000 cells were resuspended in 3 ml of semi-solid culture medium. The prepared medium with cells was then plated in triplicate into Petri dishes, each with a central circle of 35 mm diameter, filled with sterile water to prevent dehydration.

After 12 days of culture, the colonies were enumerated, and sorting was performed based on colony morphology. This methodology allowed for the quantification and classification of colonies formed by the harvested cells, providing insights into their clonogenic potential and differentiation capacity.

Flow cytometry

The expression of CD34 and CD38 surface markers on hematopoietic stem cells (HSCs) was assessed using flow cytometry. The following antibodies were utilized: CD34-PE (eBioscience) and CD38-FITC (eBioscience). Unstained controls were also prepared for all experiments to account for background fluorescence.

For each sample, 10,000 to 50,000 cells were stained with anti-CD34 FITC and CD38 PE antibodies. Subsequently, measurements were conducted using a BD FACSCalibur Flow Cytometry system. The acquired data were analyzed using FLOWJO Software, allowing for the determination of the expression levels of CD34 and CD38 on the surface of HSCs. This analysis provides valuable insights into the phenotype and potential differentiation status of the harvested cells.

Statistical Analysis

The data are presented as mean ± standard deviation (SD) or ± standard error (SE), as appropriate. Statistical comparisons between different groups were assessed using one-way ANOVA, followed by the Tukey-Kramer post-hoc test for multiple comparisons. GraphPad Prism version 7.00 was employed for statistical analysis.

The porosity of the demineralized bone matrix (DBM) was measured using Image J software version 12. Gene expression data analysis was conducted using StepOne Software v2.3.

For all statistical analyses, a significance level of $p < 0.05$ was considered statistically significant, indicating differences between groups. This threshold ensured robust interpretation of the results and identification of meaningful trends or effects within the data.

Results

Microfluidic device microfabrication

Analysis of the microchip under microscopy revealed that the scaffold was appropriately positioned inside the co-culture chamber, allowing for efficient circulation of the cell culture medium inside and around the scaffold. The perfusion flow rate played a critical role in the microfluidic culture system, with a pump ensuring fluid flow accuracy to within 1.6 µl min − 1. Specifically, a flow rate of 1.6 µl min − 1 was designated for hematopoietic stem cells (HSCs), while a flow rate of five µl min − 1 was allocated for mesenchymal stem cells (MSCs). Additionally, a range of 1.6 to 8.3 µl min − 1 was chosen to establish a dynamic culture system.

The selection of flow rates was informed by the viability assessment of cells harvested from the scaffold after three days of co-culture using trypan blue staining. Figure 1a depicts a schematic representation of the designed microfluidic device.

Characterization of MSCs and HSCs

Adherent mesenchymal stem cells (MSCs) exhibited a spindle-like morphology across all study groups (Fig. 2b). Subsequent staining with alizarin red and oil red O, as depicted in Fig. 2c and d respectively, revealed osteogenic and adipogenic differentiation of MSCs after 16 days in traditional 24-well culture. Flow cytometric analysis was conducted to characterize the early MSC phenotype, revealing that 78.93% (sd = 2.99) and 96.02% (sd = 0.66) of the cells expressed CD105 and CD90 surface markers, respectively (Data not shown). The CD45 surface marker was assessed as a negative control CD marker.

The morphology of hematopoietic stem cells (HSCs) appeared normal, exhibiting a round and non-adhesive phenotype (Fig. 2a). The purity of HSCs was evaluated by flow cytometry, demonstrating a mean purity of 50.48% (sd = 3.40) on day one, with a viability of at least 86% as estimated by trypan blue staining.

The phenotype of HSCs and MSCs on DBM scaffold

Mesenchymal stem cells (MSCs) play a crucial role in providing a niche for hematopoietic stem cells (HSCs), thereby enhancing HSCs' survival and proliferation. The phenotypes and interactions between HSCs and MSCs were investigated using electron microscopy. Scanning electron microscopy (SEM) analysis of the demineralized bone matrix (DBM) scaffold after seeding MSCs in both 3D dynamic and static groups revealed that, after three days, the scaffold spaces were filled with elongated, spindle-shaped MSCs. The extracellular matrix (ECM) produced by MSCs was visualized using inverted microscopy (marked with * in Fig. 3E, F), and MSCs completely covered the scaffold surface. Moreover, MSCs formed bridges by extending pseudopodia, as depicted in Fig. 3.

Physical interactions between round-shaped HSCs and MSCs were observed (Fig. 3b). After seven days, MSCs maintained the adhesion of HSCs to the stromal layer and ECM. HSCs exhibited strong physical interactions with the stromal layer in both experimental groups. However, in the 3D dynamic group, HSCs were surrounded by MSCs and penetrated beneath the stromal layer, whereas in the 3D static group, most

cells were present on the surface (Fig. 3c, d). Analysis using Image J software revealed that the scaffold's porosity was approximately 40% (Fig. 3a).

The enumeration of $CD34^{+}$, $CD38^{-}$ CB-HSCs on the DBM scaffold

The enumeration of harvested cells showed no statistically significant difference between day one and day seven in both the 3D dynamic and static groups (ns $p > 0.05$) (Fig. 4C). In the 3D dynamic group, the mean number of HSCs increased from approximately 10,000 to 14,000 (1.4-fold, ns $p = 0.10$, SE = 2000) at 7 days. Similarly, in the 3D static group, it increased from approximately 10,000 to 19,800 (1.9-fold, ns $p = 0.20$, SE = 4917). These results indicated a slight increase in the number of cells in the 3D static culture compared to the dynamic group.

Flow cytometry analysis qualitatively identified the phenotype of these cells, revealing differences in the distributions of CD34 + and CD38- HSCs between the 3D dynamic and 3D static groups at 1 and 7 days after HSCs co-culture. The expression of the CD34 surface marker in HSCs was 50.48% (sd = 3.40) on the first day. By the seventh day, the expression of the CD34 marker in the microfluidic 3D dynamic group increased to 72.83% (*$p = 0.02$, sd = 9.01), while in the 3D static group, the number of CD34 + HSCs was 60.33% (ns, sd = 11.59).

CD34+, CD38- cells represent a quiescent sub-population of HSCs. The highest proportion of CD34+, CD38- cells was observed in the 3D dynamic group after seven days (30.31%, SE = 1.35), whereas in the 3D static group, 16.67% (SE = 1.60) of HSCs showed CD34+, CD38- surface expression. The expression level of CD34+, CD38- in the 3D dynamic group was nearly twofold greater than in the 3D static group (1.8-fold). These results were consistent with a study conducted by Siebe et al. (CD34+, CD38- 31.7% after 28 days) in a microfluidic bone marrow chip model(27).

The number of CD34+, CD38- HSCs was statistically significant between the two groups (*$p = 0.02$). In contrast to CD34+, CD38- markers, the number of HSCs expressing CD38 + and CD34- increased significantly in the 3D static group compared to the 3D dynamic group (about 1.5-fold). The results of the flow cytometry analysis are summarized in Fig. 4A, B.

Effect of DBM on the expression of CXCR4 and RUNX1 genes.

The CXCR4/SDF-1 alpha axis plays a crucial role in the trafficking of HSCs(36). Gene expression analysis revealed distinct gene expression profiles in HSCs, particularly in terms of CXCR4 expression. CXCR4 gene expression was evaluated on days 1 and 7 after MSCs seeding in both groups. In the 3D dynamic group, CXCR4 expression increased approximately 4.7-fold over seven days. Similarly, in the 3D static group, CXCR4 gene expression increased by 3.5-fold compared to day one. The comparison of gene expression between the two 3D groups was statistically significant (*$p = 0.03$, SE = 0.35) (Fig. 4D).

The expression of the RUNX2 gene was analyzed to assess the osteogenesis potency of the DBM in the microfluidic co-culture system. After three days, adherent MSCs were isolated, and RUNX2 gene

expression was evaluated. The expression of RUNX2 mRNA was significantly increased by 9.4-fold (± 0.72) in the 3D dynamic group compared to the control group (****$p < 0.001$, SE = 0.37). These results indicate the enhanced osteogenic potential of the DBM scaffold in the microfluidic co-culture system.

Figure 4: Illustration of the expression of CD34 and CD38 surface markers, the expression of CXCR4, RUNX2 genes, as well as colony-forming potency between the 3D dynamic and 3D static groups. (a) Flow cytometry analysis depicting the expression levels of CD34 and CD38 on the surface of HSCs. (b) Mean expression levels of CD markers in different experimental groups. (c) Total harvested cell counts in the study groups and their changes between the first and seventh days. (d, e) Relative expression levels of CXCR4 and RUNX2 genes, (f) HSCs multilineage differentiation potency.

HSCs multilineage differentiation potency

The multilineage differentiation potency of harvested HSCs was assessed using a colony-forming units assay in both the 3D dynamic and static groups. The analysis revealed that the total colony number of HSCs derived from the 3D static group increased by 2.8-fold (± 0.8) compared to the control after 12 days. Similarly, in the 3D dynamic group, the number of CFUs increased by 3.6-fold (± 1.08) compared to the control (Fig. 4f). However, the data did not show statistical significance between the two groups.

Discussion

One of the key challenges in utilizing cord blood HSCs for bone marrow transplantation (BMT) is the limited number of CD34 + cells. Clinical outcomes have indicated that successful engraftment correlates with higher numbers of CD34 + cells (5, 37, 38). Recent clinical trials have underscored the importance of developing effective methods for expanding HSCs in vitro, potentially overcoming the limitations associated with cord blood HSC numbers for adult BMT. Various approaches have been explored to enhance HSC expansion(8, 39–42). It has been suggested that recreating an environment closely resembling the native HSC niche is crucial for successful ex vivo expansion of HSCs. However, while HSC fate is intricately regulated within its niche in vivo, engineering a suitable HSC niche for in vitro expansion poses several challenges.In this study, we present a novel microfluidic-based 3D dynamic co-culture system designed to maintain HSCs in a dormant state under cytokine-free conditions. Utilizing DBM as a scaffold, MSCs were seeded to create a supportive feeder layer on the scaffold. Our findings indicate that the microfluidic co-culture approach led to an increased number of CD34 + HSCs compared to the dynamic group. This suggests the potential of our system to promote the expansion of CD34 + HSCs, highlighting its utility in stem cell research and therapeutic applications.

HSCs are intricately regulated by both intrinsic and extrinsic signals within the niche, which is crucial for maintaining hematopoietic homeostasis(43). This niche comprises stromal cells, ECM and interstitial fluid, providing a specialized 3D environment for HSCs in vivo. We hypothesized that the interplay between HSCs, mesenchymal stem cells (MSCs), and ECM proteins through direct and indirect crosstalk could enhance HSCs expansion.

Recent advancements in live imaging techniques have shed light on the importance of direct interactions between HSCs and stromal cells in maintaining HSCs within the niche. MSCs, in particular, play a pivotal role in HSCs self-renewal and bone remodeling regulation(44). These versatile cells have the capability to differentiate into various cell types within the bone marrow, including osteoblasts, which are essential for creating the bone microenvironment and regulating HSCs dormancy(45).

A growing body of evidence suggests that MSCs or MSCs-derived cells can physically attach to HSCs (45, 46). Our analysis of scanning electron microscopy results revealed distinct interactions between MSCs and HSCs in both 3D dynamic and static culture conditions. In the 3D dynamic group, HSCs were observed to be located beneath the MSCs feed layer, whereas in the 3D static group, HSCs were predominantly situated on the surface layer of MSCs. Notably, MSCs in the 3D dynamic group surrounded the HSCs in sheaths by forming pseudopodia, as depicted in Fig. 3. These findings are consistent with previous studies, such as the work conducted by Duohui Jing et al., which demonstrated that CD34 + quiescent HSCs could penetrate beneath the layer of MSCs(20). In dynamic cell culture conditions, HSCs retained their stemness capacity by penetrating the underlying layer formed by MSCs. Flow cytometry and colony assay results further confirmed the stemness ability of CD34 + HSCs, as illustrated in Fig. 4.

The CXCR4 gene expression was investigated to elucidate the potential mechanism underlying the traffic of HSCs beneath the MSCs layer. This trafficking process is contingent upon the expression of specific chemotactic genes, including CXCR4, which facilitate HSCs migration within the bone marrow niche(36). In the bone marrow microenvironment, stromal-derived factor 1 alpha (SDF-1α) binds to the CXCR4 receptor, thereby regulating HSCs quiescence and trafficking. Various cell types within the bone marrow, including CXCL12-abundant reticular (CAR) cells, osteoblasts, endothelial cells, osteocytes, and MSCs, have been reported to secrete SDF-1α, thereby contributing to the chemotactic gradient guiding HSCs movement. Our analysis revealed a significant difference in CXCR4 gene expression between the 3D dynamic and static groups (Fig. 4d), suggesting that MSCs may induce CXCR4 expression in the 3D dynamic culture environment. It is worth noting that while the CXCR4/SDF-1 axis is considered the primary signaling pathway governing HSCs trafficking, other pathways also contribute to this process. The higher expression of the CXCR4 gene in expanded HSCs implies the potential suitability of these cells for transplantation. However, it is essential to acknowledge that the analysis presented here only examines gene expression levels, and further investigations are warranted to determine whether this gene expression translates into protein production, considering potential post-translational modifications.

MSCs derived ECM is actively produced in the 3D dynamic and static group (marked with * symbol in Fig. 3e, F). ECM proteins influence HSCs differentiation, lineage specification, proliferation, and cell death(47). ECM is a meshed structure of proteins (such as collagen, fibronectin, laminin) that acts as a cytokine reservoir. This network attaches directly to HSCs(48, 49). Various studies have shown that it has a vital role in the proliferation and differentiation of HSCs(50). Natural cytokines produced under a 3D dynamic co-culture group are available to all HSCs due to perfusion flow. The MSCs derived ECM acts as an excellent reservoir for the storage of these cytokines. The Flow cytometry results showed that after

seven days of co-culture, HSCs showed higher expression of CD34 surface markers in 3D culture. Enhanced HSCs ability to self-renewal was showed in the colony assay. These results indicate that MSCs are needed for self-renewal, maintenance of stemness, and proliferation of HSCs. The condition of the co-culture in our study was without cytokines. We assume that MSCs, through direct physical contact and actively regular production of cytokines and ECM, are causing HSCs expansion. Interestingly, these variables were higher in microfluidic 3D co-culture than in static three-dimensional culture, which shows the positive role of laminar fluid flow in the microfluidic system than traditional static culture. Here, we did not directly measure the change in cytokines or ECM proteins, But Schmal and et al. showed that MSCs synthetizing niche-specific ECM components in a hanging drop model(51).

The production of MSCs-derived extracellular matrix (ECM) was observed in both the 3D dynamic and static groups, as indicated by the * symbol in Fig. 3e, f. ECM proteins play a crucial role in influencing various aspects of HSCs biology, including differentiation, lineage specification, proliferation, and cell survival. ECM, composed of proteins such as collagen, fibronectin, and laminin, forms a meshed structure that serves as a reservoir for cytokines. This network directly interacts with HSCs, affecting their behavior and fate.

Many studies have reported that HSCs can be expanded ex-vivo in certain conditions (52, 53). Conventionally, these methods have focused on the cytokine cocktail. Many cytokine cocktails for ex-vivo expansion of HSCs has been described (26) but suffer from some severe disadvantages (54). In essence, cytokines are necessary but insufficient for quality expansion of HSCs multiplication ex-vivo. Also, Prior studies have less noted the importance of 3D topology and microenvironment on HSCs fate. 3D culture has been one of the most significant leaps in HSCs expansion, and it established a new approach for mimicking HSCs niche.

The results of flow cytometry showed that three-dimensional culture significantly increased the portion of $CD34^{+}$, $CD38^{-}$ HSCs compared to two-dimensional. 3D culture creates a remarkable similarity between ex-vivo culture and natural niche. Tan et al. results indicated that the 3D scaffold led to a five to seven-fold increase in the frequency of LTC-IC numbers over 14 days of culture, significantly higher than in 2D control culture(55). In conventional 2D culture, cells grow on monolayer and only one side of the flask. Usual monolayer expanding methods enhanced HSCs differentiation (56). Therefore, it seems necessary to imitate HSCs 3D natural niche to reduce HSCs differentiation and improve HSCs expansion.

Shifting from a two-dimensional to a three-dimensional cell culture system requires a scaffold (57). Scaffold and spatial, specifically BM structure, have been a subject of significant interest in recent years. Many studies have been carried out to in vitro expansion of HSCs by co-culture method [18–20] such as PEG hydrogel (58, 59), fibrin scaffold (60), collagen(61). However, a few have also paid attention to the physical structure of the cell microenvironment. Scaffolds can be closely mimicking the three-dimensional environments of the HSCs niche. We showed DBM as a 3D natural bone marrow scaffold that has provided a suitable layer (ex: high porosity, native scaffold) for crosstalk between HSCs and MSCs. DBM is comprised of 93% collagen type I and various growth factors(62). Collagen is the main

protein found in bone marrow ECM(47). Collagen gel scaffolds based can help to improve $CD34^+$ HSCs reconstitution(37). Natural DBM scaffold is easy to make; it is widely available and composed of natural ECM (33). SEM images and invert microscopy show that MSCs are repopulated on the DBM surface and migrated through the scaffold (Fig. 4). DBM scaffold has a porous surface (Fig. 4A). The mean porosity of the DBM scaffold was 33.7%. It allows DBM to penetrate cells, whereas synthetic compositions such as nanofibers do not simulate such conditions. The main feature of the natural essence of the cellular microenvironment is 3D architecture. The red bone marrow that within the normal hematopoiesis take place is located in the trabecular bone area. Trabecular bone or cancellous bone has a highly porous structure, which provides many factors that make it suitable for maintenance of the hematopoietic compartment. The number of CFU between the 3D dynamic and static group was not significant. It has already been reported that the number of colonies in the collagen scaffold is less than other scaffolds(63).

Flow cytometric analysis and cloning assays revealed notable differences in cell phenotypes between dynamic and static cultures. Specifically, CD34+, CD38- HSCs exhibited a 1.8-fold increase in the 3D dynamic culture compared to the 3D static group. Interestingly, the count of CD34 + cells decreased in the 3D static group, with a significant reduction observed in the 2D static group. The CD34+, CD38- subpopulation of HSCs is clinically relevant for bone marrow transplantation, as these cells possess high proliferative potential. The microfluidic co-culture system demonstrated superior potential for maintaining stemness in HSCs, as evidenced by the higher proportion of CD34 + positive and CD38- negative cells compared to static three-dimensional culture.In the 3D static group, a higher number of more differentiated cells, characterized by CD38 and CD34 double-positivity, was observed, indicating a bias towards differentiation in this culture condition. In contrast, the 3D dynamic microfluidic group favored a self-renewal phenotype, as indicated by a higher proportion of undifferentiated CD34 + cells. These findings align with previous research(31) and highlight the impact of culture conditions on HSC differentiation and self-renewal dynamics.

While both quantitative (harvested cell count) and qualitative (flow cytometric) analyses suggested a dormant phenotype in the microfluidic system, colony assays were conducted to assess the functional potency of HSCs. Consistent with previous findings (27), the dynamic 3D culture supported not only differentiation but also the ability to differentiate into all precursor cells. However, it is important to note that functional in vivo assays for HSC activity post-co-culture were not performed in this study.

Although the expansion of CD34 + HSCs in the microfluidic 3D co-culture was lower compared to other reports, our results demonstrated higher purity of CD34 + CD38- HSCs in the microfluidic 3D co-culture. This suggests that the microfluidic system may offer advantages in preserving the stemness and purity of HSC populations, despite lower overall expansion levels.

Unlike traditional co-culture systems, microfluidic systems offer several advantages by providing cells with nutrients and oxygen while continuously removing waste from the environment. The perfusion flow in microfluidic systems ensures the homogeneous distribution of cytokines throughout the culture area,

making them readily available to all cells. Additionally, microfluidic systems can mimic physiological conditions such as blood flow and shear stress, which are crucial for better simulating bone marrow stimulation in vitro compared to static co-culture systems.

The interstitial fluid in the bone marrow creates biomechanical signaling(64), and niche cells respond to mechanical signals such as shear stress and mechanical forces. In the cytokine-free dynamic co-culture group, the results indicate that chemokines and other signaling molecules provided by MSCs were effectively delivered to all cells due to the perfusion flow. This resulted in an increase in the number of CD34 + HSCs. Comparing the 3D dynamic and static groups, it was observed that HSCs in the dynamic co-culture system were more likely to enter a dormant state due to the influence of perfusion flow.

We hypothesize that the 3D co-culture environment induces the differentiation of MSCs into osteoblasts. To investigate this hypothesis, we analyzed the expression of the RUNX2 gene, which is a key regulator of osteoblast differentiation. Our results revealed that MSCs exhibited significantly higher expression of the RUNX2 gene in the 3D dynamic culture compared to the culture without a scaffold. Additionally, the presence of the DBM scaffold further enhanced the expression of the RUNX2 gene in MSCs. Previous studies have shown that fluid flow in microfluidic environments can induce the expression of osteogenic genes such as Runx2(65).

These findings suggest that the DBM scaffold possesses inherent osteogenic properties, and the presence of fluid flow enhances MSC differentiation into osteoblasts. Increased expression of the RUNX2 gene in MSCs is indicative of osteoblast differentiation. Given that quiescent HSCs are often located in the endosteal niche, where bone-forming osteoblasts play a crucial role in supporting HSCs, the differentiation of MSCs into osteoblastic lineage brings the 3D dynamic co-culture system closer to mimicking the in vivo endosteal niche.

Direct physical interactions between HSCs and osteoblast cells have been documented in previous studies(66). Thus, the co-culture of HSCs and MSCs in the DBM scaffold maintains the stemness properties of HSCs by promoting the differentiation of MSCs into osteoblastic cells, thereby creating a microenvironment that resembles the endosteal niche.

Conclusion

In summary, our study demonstrates that the microfluidic-based 3D co-culture model utilizing the DBM scaffold with stromal support can effectively maintain HSCs' self-renewal in cytokine-free conditions. This innovative approach provides a three-dimensional structure for the HSC niche, incorporating feeder layer cells, thereby offering a novel strategy for expanding HSCs in vitro. By mimicking bone marrow cell-cell interactions in a 3D culture, our model exhibits features that closely resemble the realistic bone marrow environment compared to conventional 2D culture systems. The integration of microfluidic flow with a natural 3D scaffold enables the simulation of key aspects of the bone marrow niche. We believe that our findings hold promise in addressing the limitations associated with umbilical cord blood HSCs

expansion in vitro and could potentially be applied to the development of novel concepts in personalized medicine, such as bone marrow-on-chip platforms.

Declarations

Ethics approval and consent to participate

Not applicable

Consent for publication

Not applicable

Availability of data and materials

Not applicable. If your manuscript does not contain any data, please state 'Not applicable' in this section.

Conflict of interest

The authors declare that they have no competing interests

Funding

Support was given by the Tarbiat Modares University, who funded the work in all its stages.

Author Contribution Statement

Data curation, A.A. and M.A.; Formal analysis, A.A. and A.A.; Preparing figures, A.A.; Funding acquisition, M.S.; Project administration, M.S.; Writing—original draft, A.A.; Writing—review & editing, AA. and M.S.

References

1. Ng, A. P. & Alexander, W. S. Haematopoietic stem cells: Past, present and future. *Cell Death Discovery* (2017) doi:10.1038/cddiscovery.2017.2.
2. Eaves, C. J. Hematopoietic stem cells: Concepts, definitions, and the new reality. *Blood* (2015) doi:10.1182/blood-2014-12-570200.
3. Dzierzak, E. & Bigas, A. Blood Development: Hematopoietic Stem Cell Dependence and Independence. *Cell Stem Cell* (2018) doi:10.1016/j.stem.2018.04.015.
4. Gratwohl, A. *et al.* Hematopoietic stem cell transplantation: A global perspective. *JAMA - J. Am. Med. Assoc.* (2010) doi:10.1001/jama.2010.491.
5. Heimfeld, S. Bone marrow transplantation: how important is CD34 cell dose in HLA-identical stem cell transplantation? *Leukemia* **17**, 856–8 (2003).

6. Takagi, S. *et al.* Cord Blood Units Containing Lower CD34+ Cells (0.5 - 1.0 x 105 /kg) Could be Alternative Donor Candidates for Single-Unit Cord Blood Transplantation for Adults: A Retrospective Study of 421 Patients in a Single Institute. *Blood* **132**, 2089 (2018).
7. Kelly, S. S., Sola, C. B. S., de Lima, M. & Shpall, E. Ex vivo expansion of cord blood. *Bone Marrow Transpl.* **44**, 673–681 (2009).
8. Flores-Guzmán, P., Fernández-Sánchez, V. & Mayani, H. Concise Review: Ex Vivo Expansion of Cord Blood-Derived Hematopoietic Stem and Progenitor Cells: Basic Principles, Experimental Approaches, and Impact in Regenerative Medicine. *Stem Cells Transl. Med.* **2**, 830–838 (2013).
9. Yamamoto, H. Single cord blood transplantation in Japan; expanding the possibilities of CBT. *Int. J. Hematol.* (2019) doi:10.1007/s12185-019-02672-4.
10. Aljurf, M. *et al.* "Worldwide Network for Blood & Marrow Transplantation (WBMT) special article, challenges facing emerging alternate donor registries". *Bone Marrow Transplantation* (2019) doi:10.1038/s41409-019-0476-6.
11. Ballen, K. K., Gluckman, E. & Broxmeyer, H. E. Umbilical cord blood transplantation: the first 25 years and beyond. *Blood* (2013) doi:10.1182/blood-2013-02-453175.
12. Wagner, J. E. *et al.* One-Unit versus Two-Unit Cord-Blood Transplantation for Hematologic Cancers. *N. Engl. J. Med.* (2014) doi:10.1056/NEJMoa1405584.
13. Bornstein, R. *et al.* A Modified Cord Blood Collection Method Achieves Sufficient Cell Levels for Transplantation in Most Adult Patients. *Stem Cells* (2005) doi:10.1634/stemcells.2004-0047.
14. Sumide, K. *et al.* A revised road map for the commitment of human cord blood CD34-negative hematopoietic stem cells. *Nat. Commun.* (2018) doi:10.1038/s41467-018-04441-z.
15. Berz, D., McCormack, E. M., Winer, E. S., Colvin, G. A. & Quesenberry, P. J. Cryopreservation of hematopoietic stem cells. *American Journal of Hematology* (2007) doi:10.1002/ajh.20707.
16. Andrade-Zaldívar, H., Santos, L. & De León Rodríguez, A. Expansion of human hematopoietic stem cells for transplantation: trends and perspectives. *Cytotechnology* **56**, 151–160 (2008).
17. Tajer, P., Pike-Overzet, K., Arias, S., Havenga, M. & Staal, F. Ex Vivo Expansion of Hematopoietic Stem Cells for Therapeutic Purposes: Lessons from Development and the Niche. *Cells* (2019) doi:10.3390/cells8020169.
18. Takizawa, H., Schanz, U. & Manz, M. G. Ex vivo expansion of hematopoietic stem cells: mission accomplished? *Swiss Med Wkly* **141**, w13316 (2011).
19. Mehta, R. S. *et al.* Novel techniques for Ex vivo expansion of cord blood: Clinical trials. *Frontiers in Medicine* (2015) doi:10.3389/fmed.2015.00089.
20. Maung, K. K. & Horwitz, M. E. Current and future perspectives on allogeneic transplantation using ex vivo expansion or manipulation of umbilical cord blood cells. *Int. J. Hematol.* (2019) doi:10.1007/s12185-019-02670-6.
21. Wei, Q. & Frenette, P. S. Niches for Hematopoietic Stem Cells and Their Progeny. *Immunity* (2018) doi:10.1016/j.immuni.2018.03.024.

22. Boulais, P. E. & Frenette, P. S. Making sense of hematopoietic stem cell niches. *Blood* **125**, 2621–2629 (2015).
23. Raic, A., Naolou, T., Mohra, A., Chatterjee, C. & Lee-Thedieck, C. 3D models of the bone marrow in health and disease: Yesterday, today, and tomorrow. *MRS Communications* (2019) doi:10.1557/mrc.2018.203.
24. Battiwalla, M. & Hematti, P. Mesenchymal stem cells in hematopoietic stem cell transplantation. *Cytotherapy* **11**, 503–515 (2009).
25. Caplan, A. I. Chapter 29 - Mesenchymal Stem Cells. in *Essentials of Stem Cell Biology (Second Edition)* (ed. Wilmut, R. L. G. H. M. P. D. T. T.) 243–248 (Academic Press, 2009). doi:http://dx.doi.org/10.1016/B978-0-12-374729-7.00029-9.
26. Aggarwal, S. & Pittenger, M. F. Human mesenchymal stem cells modulate allogeneic immune cell responses. *Blood* **105**, 1815–1822 (2005).
27. Jing, D. *et al.* Hematopoietic stem cells in co-culture with mesenchymal stromal cells--modeling the niche compartments in vitro. *Haematologica* **95**, 542–550 (2010).
28. Kräter, M. *et al.* Bone marrow niche-mimetics modulate HSPC function via integrin signaling. *Sci. Rep.* (2017) doi:10.1038/s41598-017-02352-5.
29. Cowin, S. C. & Cardoso, L. Blood and interstitial flow in the hierarchical pore space architecture of bone tissue. *J. Biomech.* (2015) doi:10.1016/j.jbiomech.2014.12.013.
30. Warren, S. M. *et al.* A novel flow-perfusion bioreactor supports 3D dynamic cell culture. *J. Biomed. Biotechnol.* (2009) doi:10.1155/2009/873816.
31. Torisawa, Y. *et al.* Bone marrow–on–a–chip replicates hematopoietic niche physiology in vitro. *Nat Meth* **11**, 663–669 (2014).
32. Nielsen, L. K. Bioreactors for hematopoietic cell culture. *Annu Rev Biomed Eng* **1**, 129–152 (1999).
33. Sauvageau, G., Iscove, N. N. & Humphries, R. K. In vitro and in vivo expansion of hematopoietic stem cells. *Oncogene* **23**, 7223–7232 (2004).
34. Sieber, S. *et al.* Bone marrow-on-a-chip: Long-term culture of human haematopoietic stem cells in a three-dimensional microfluidic environment. *J. Tissue Eng. Regen. Med.* (2018) doi:10.1002/term.2507.
35. McNiece, I., Robinson, S. & Shpall, E. MSC for Ex Vivo Expansion of Umbilical Cord Blood Cells. in *Mesenchymal Stromal Cells* (eds. Hematti, P. & Keating, A.) 485–501 (Springer New York, 2013). doi:10.1007/978-1-4614-5711-4_27.
36. Ehring, B. *et al.* Expansion of HPCs from cord blood in a novel 3D matrix. *Cytotherapy* (2003) doi:10.1080/14653240310003585.
37. Meretzki, S. *et al.* Expansion of Hematopoietic Stem Cells (HSC) from Cord-Blood (CB) Derived Mononuclear Cells (MNC) in Cytokine-Free Environment Using Mesenchymal Cells Spatial Co-Culture System. *Blood* **108**, 2565 LP – 2565 (2015).

38. Chou, D. B. *et al.* On-chip recapitulation of clinical bone marrow toxicities and patient-specific pathophysiology. *Nat. Biomed. Eng.* (2020) doi:10.1038/s41551-019-0495-z.
39. Guckenberger, D. J. *et al.* A Combined Fabrication and Instrumentation Platform for Sample Preparation. *J. Lab. Autom.* **19**, 267–274 (2014).
40. Chakkalakal, D. A. *et al.* Demineralized bone matrix as a biological scaffold for bone repair. in *Tissue Engineering* (2001). doi:10.1089/107632701300062778.
41. Cho, J. S. *et al.* Isolation and characterization of multipotent mesenchymal stem cells in nasal polyps. *Exp. Biol. Med.* (2015) doi:10.1177/1535370214553898.
42. Murtey, M. Das & Ramasamy, P. Sample Preparations for Scanning Electron Microscopy – Life Sciences. in *Modern Electron Microscopy in Physical and Life Sciences* (2016). doi:10.5772/61720.
43. Leisten, I. *et al.* 3D co-culture of hematopoietic stem and progenitor cells and mesenchymal stem cells in collagen scaffolds as a model of the hematopoietic niche. *Biomaterials* **33**, 1736–1747 (2012).
44. Tse, W. & Laughlin, M. J. Umbilical cord blood transplantation: a new alternative option. *Hematology Am. Soc. Hematol. Educ. Program* **2005**, 377–83 (2005).
45. de Lima, M. *et al.* Transplantation of ex vivo expanded cord blood cells using the copper chelator tetraethylenepentamine: a phase I/II clinical trial. *Bone Marrow Transpl.* **41**, 771–778 (2008).
46. Palsson, B. O. *et al.* Expansion of human bone marrow progenitor cells in a high cell density continuous perfusion system. *Biotechnol. (N Y)* **11**, 368–372 (1993).
47. Rollini, P., Kaiser, S., Faes-van't Hull, E., Kapp, U. & Leyvraz, S. Long-term expansion of transplantable human fetal liver hematopoietic stem cells. *Blood* **103**, 1166–70 (2004).
48. Dellatore, S. M., Garcia, A. S. & Miller, W. M. Mimicking Stem Cell Niches to Increase Stem Cell Expansion. *Curr. Opin. Biotechnol.* **19**, 534–540 (2008).
49. Di Maggio, N. *et al.* Toward modeling the bone marrow niche using scaffold-based 3D culture systems. *Biomaterials* **32**, 321–329 (2011).
50. Kirouac, D. C. *et al.* Cell-cell interaction networks regulate blood stem and progenitor cell fate. *Mol. Syst. Biol.* (2009) doi:10.1038/msb.2009.49.
51. Mendez-Ferrer, S. *et al.* Mesenchymal and haematopoietic stem cells form a unique bone marrow niche. *Nature* **466**, 829–34 (2010).
52. Pinho, S. & Frenette, P. S. Haematopoietic stem cell activity and interactions with the niche. *Nature Reviews Molecular Cell Biology* (2019) doi:10.1038/s41580-019-0103-9.
53. Asri, A., Sabour, J., Atashi, A. & Soleimani, M. Homing in hematopoietic stem cells: focus on regulatory role of CXCR7 on SDF1a/CXCR4 axis. *EXCLI J.* **15**, 134–143 (2016).
54. Gattazzo, F., Urciuolo, A. & Bonaldo, P. Extracellular matrix: a dynamic microenvironment for stem cell niche. *Biochim Biophys Acta* **1840**, 2506–2519 (2014).
55. Bhatia, R., Williams, A. D. & Munthe, H. A. Contact with fibronectin enhances preservation of normal but not chronic myelogenous leukemia primitive hematopoietic progenitors. *Exp. Hematol.* **30**, 324–

332 (2002).

56. Hynes, R. O. Extracellular matrix: not just pretty fibrils. *Science* **326**, 1216–1219 (2009).
57. Zhang, P. *et al.* The physical microenvironment of hematopoietic stem cells and its emerging roles in engineering applications. *Stem Cell Research and Therapy* (2019) doi:10.1186/s13287-019-1422-7.
58. Schmal, O. *et al.* Hematopoietic Stem and Progenitor Cell Expansion in Contact with Mesenchymal Stromal Cells in a Hanging Drop Model Uncovers Disadvantages of 3D Culture. *Stem Cells Int.* **2016**, (2016).
59. Wilkinson, A. C. *et al.* Long-term ex vivo haematopoietic-stem-cell expansion allows nonconditioned transplantation. *Nature* (2019) doi:10.1038/s41586-019-1244-x.
60. Walasek, M. A., van Os, R. & de Haan, G. Hematopoietic stem cell expansion: challenges and opportunities. *Ann N Y Acad Sci* **1266**, 138–150 (2012).
61. Tan, J. *et al.* Maintenance and expansion of hematopoietic stem/progenitor cells in biomimetic osteoblast niche. *Cytotechnology* **62**, 439–448 (2010).
62. Carletti, E., Motta, A. & Migliaresi, C. Scaffolds for tissue engineering and 3D cell culture. *Methods Mol. Biol.* **695**, 17–39 (2011).
63. Raic, A., Rödling, L., Kalbacher, H. & Lee-Thedieck, C. Biomimetic macroporous PEG hydrogels as 3D scaffolds for the multiplication of human hematopoietic stem and progenitor cells. *Biomaterials* **35**, 929–940 (2014).
64. Rödling, L. *et al.* 3D models of the hematopoietic stem cell niche under steady-state and active conditions. *Sci. Rep.* **7**, 4625 (2017).
65. Ventura Ferreira, M. S. *et al.* Cord blood-hematopoietic stem cell expansion in 3D fibrin scaffolds with stromal support. *Biomaterials* **33**, 6987–6997 (2012).
66. Blanco, T. M., Mantalaris, A., Bismarck, A. & Panoskaltsis, N. The development of a three-dimensional scaffold for ex vivo biomimicry of human acute myeloid leukaemia. *Biomaterials* **31**, 2243–2251 (2010).
67. Ho, M. S., Medcalf, R. L., Livesey, S. A. & Traianedes, K. The dynamics of adult haematopoiesis in the bone and bone marrow environment. *Br J Haematol* (2015) doi:10.1111/bjh.13445.
68. Choi, J. S. & Harley, B. A. C. Marrow-inspired matrix cues rapidly affect early fate decisions of hematopoietic stem and progenitor cells. *Sci. Adv.* (2017) doi:10.1126/sciadv.1600455.
69. Miller, S. C., de Saint-Georges, L., Bowman, B. M. & Jee, W. S. Bone lining cells: structure and function. *Scanning Microsc.* **3**, 953–60 (1989).
70. Riehl, B. & Lim, J. Macro and Microfluidic Flows for Skeletal Regenerative Medicine. *Cells* (2012) doi:10.3390/cells1041225.
71. Neiva, K., Sun, Y. X. & Taichman, R. S. The role of osteoblasts in regulating hematopoietic stem cell activity and tumor metastasis. *Brazilian Journal of Medical and Biological Research* (2005) doi:10.1590/S0100-879X2005001000001.

Figures

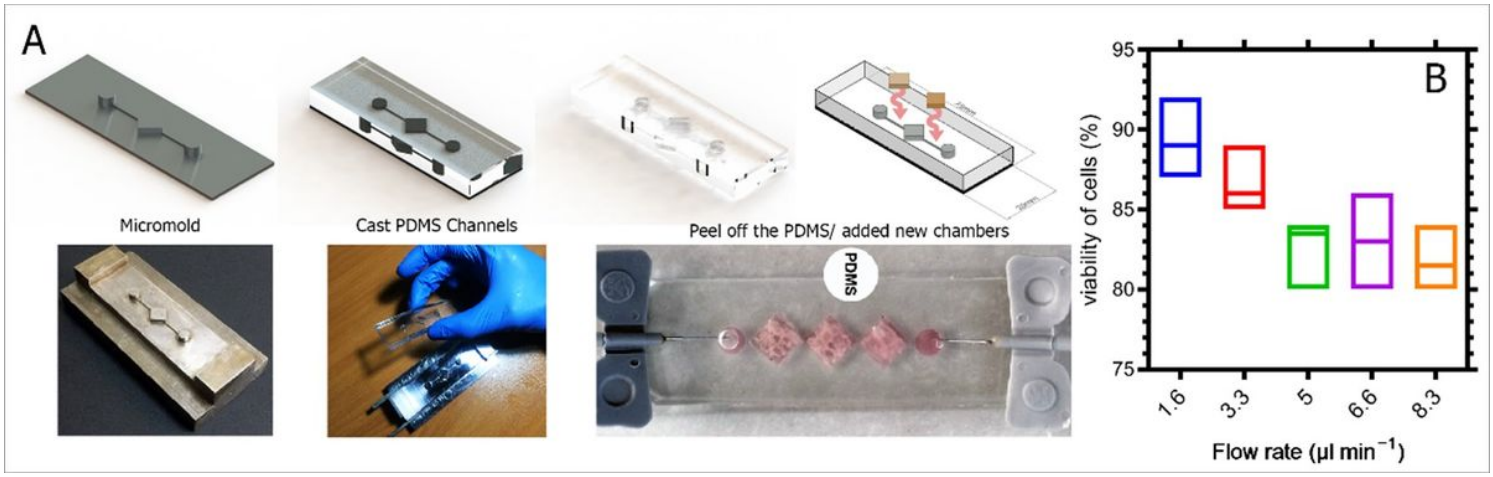

Figure 1

Design and setup of the microfluidic device. The micro-mold was fabricated using the CNC method and utilized for casting polydimethylsiloxane (PDMS) chips via soft lithography. The image illustrates three chambers within the device, designed to enhance accuracy and repeatability compared to a single chamber configuration. The dimensions of the chip were 25 mm by 75 mm, with the inlet and outlet heights exceeding those of the main culture chamber (a). The fluid flow chart and cell viability analysis indicated that at a flow rate of 1.6 µl min−1, cell viability reached 89% (89.33, sd=2.51). Evaluation was conducted solely within the range of 1.6-8.3 µl min−1 (b).

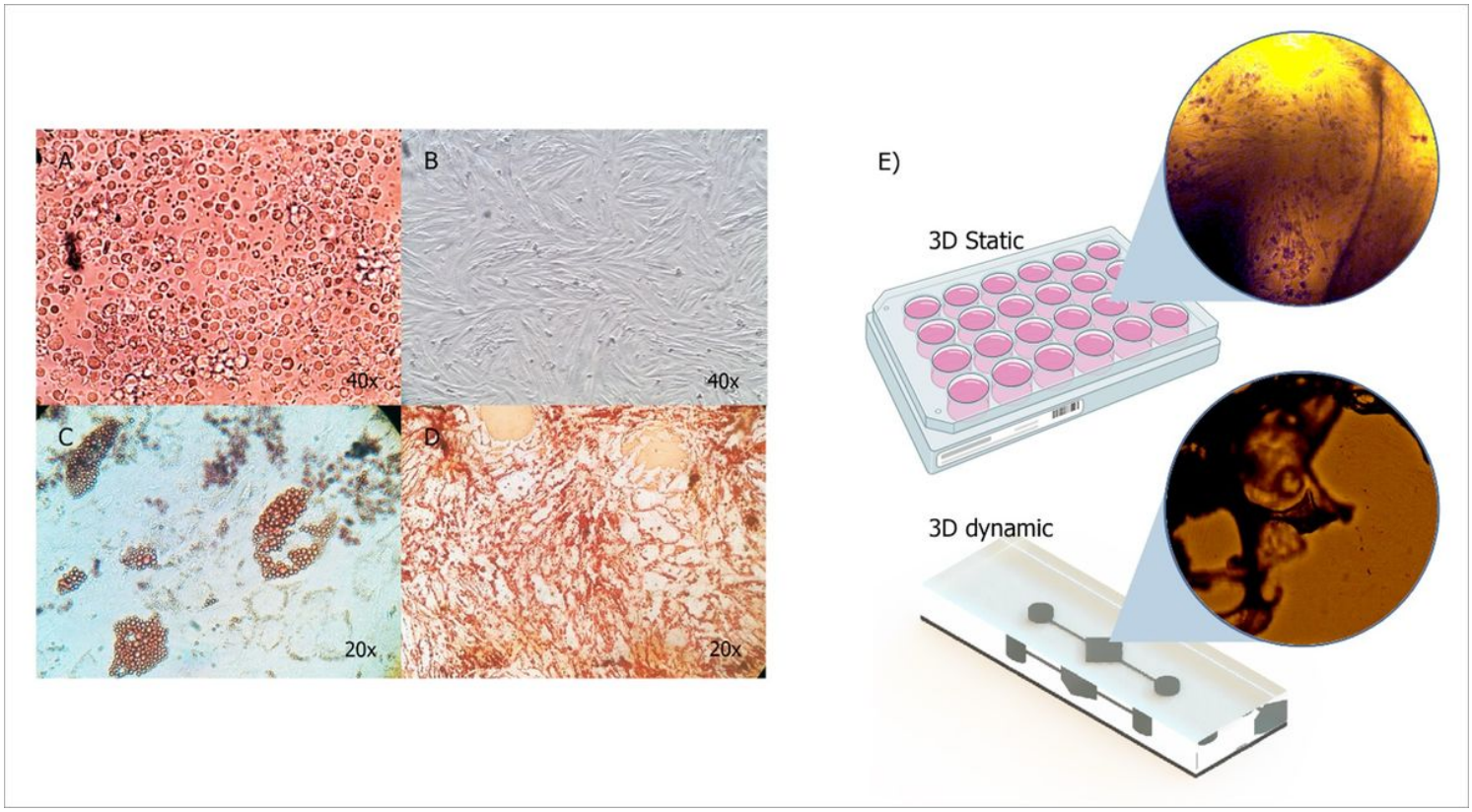

Figure 2

Morphology characterization of mesenchymal stem cells (MSCs) and hematopoietic stem cells (HSCs). (a). Spindle-like morphology of MSCs. (b). Oil red O staining demonstrating the potential of MSCs to differentiate into adipocytes. (c). Alizarin Red staining confirming the osteogenic differentiation capacity of MSCs (e) Schematic representation illustrating the morphology of HSCs and MSCs within the scaffold after seven days of co-culture.

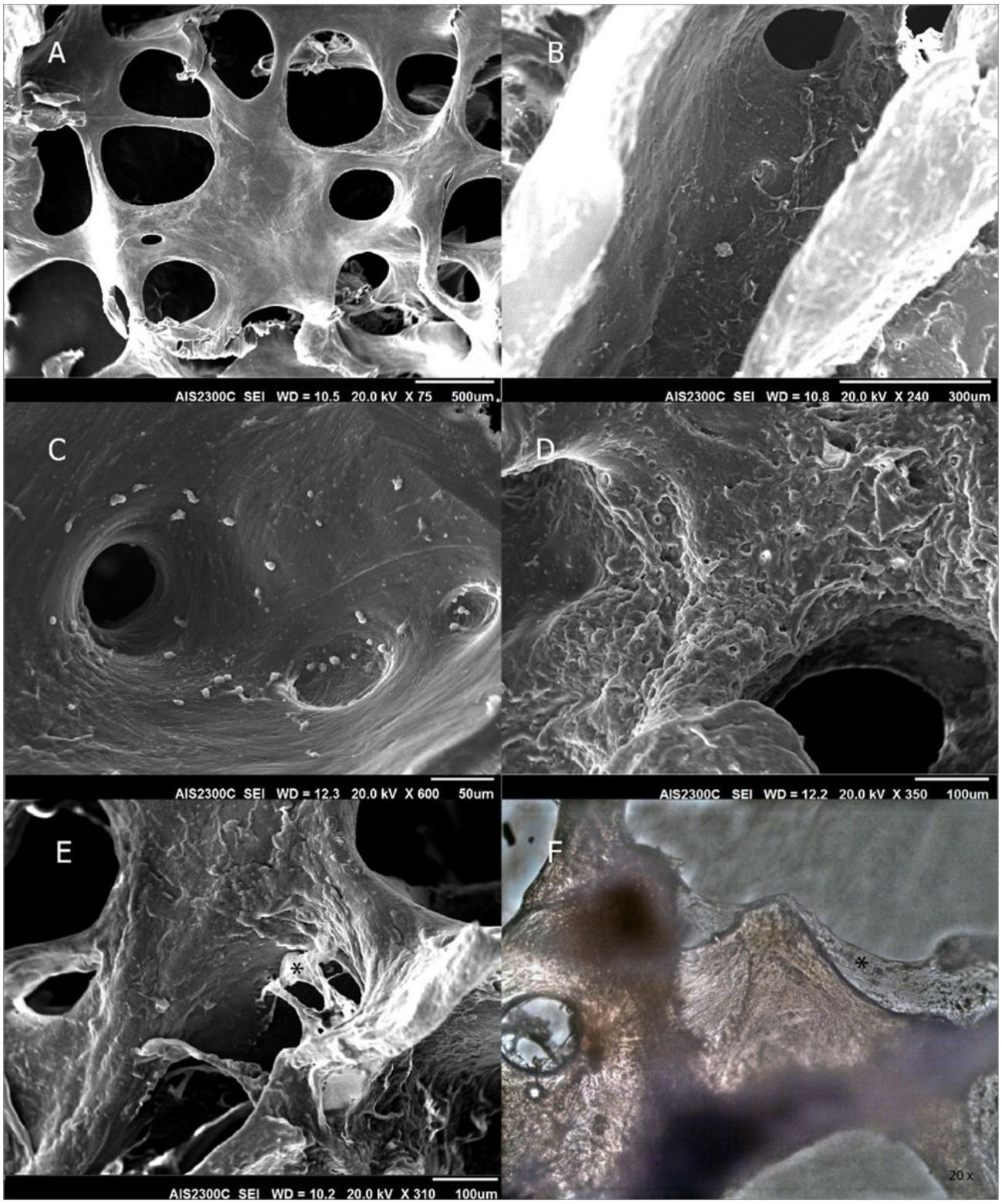

Figure 3

Cell morphology of MSCs and HSCs, and the interaction between them in electron microscopy imaging. (a) The demineralized bone matrix (DBM) exhibited porosity akin to the bone marrow, providing a spatial 3D environment conducive to mimicking the bone marrow niche. Despite its high porosity, the culture media in the microfluidic device flowed well in and around it. (b) After 48 hours, MSCs formed a stromal layer on the scaffold. The physical relationship between MSCs and HSCs is depicted in both 3D static (c) and 3D dynamic (d) groups. (e) MSCs-derived pseudopodia are observed in the 3D dynamic group. (f) ECM marked with *, is visualized under inverted microscopy.

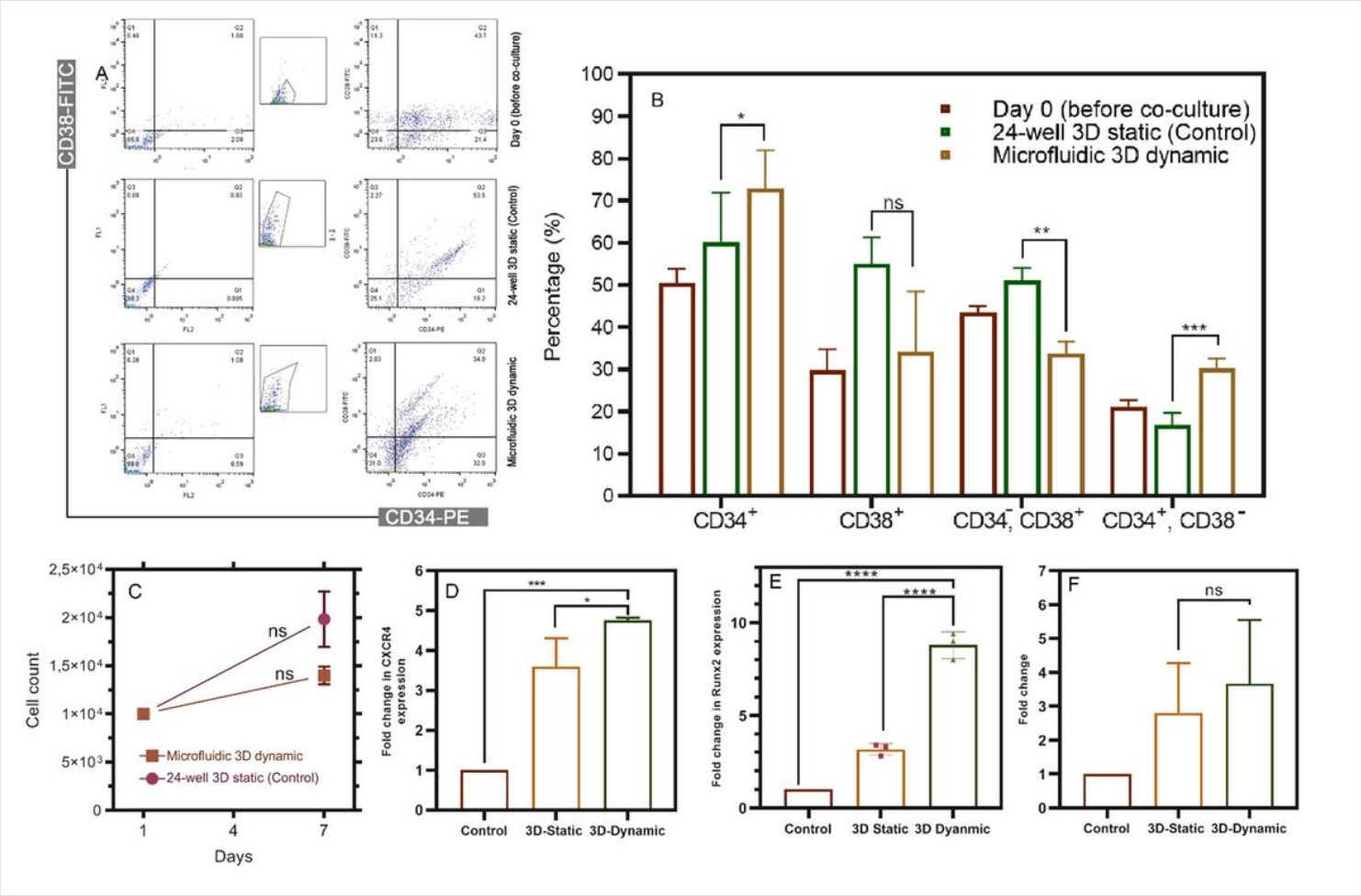

Figure 4

Illustration of the expression of CD34 and CD38 surface markers, the expression of CXCR4, RUNX2 genes, as well as colony-forming potency between the 3D dynamic and 3D static groups. (a) Flow cytometry analysis depicting the expression levels of CD34 and CD38 on the surface of HSCs. (b) Mean expression levels of CD markers in different experimental groups.(c) Total harvested cell counts in the study groups and their changes between the first and seventh days. (d, e) Relative expression levels of CXCR4 and RUNX2 genes, (f) HSCs multilineage differentiation potency.